

Simulation and Control of a PV System connected to a Low Voltage Network

J. Salazar, F. Tadeo, C. Prada, L. Palacin

Department of Systems Engineering and Automatic Control
University of Valladolid
47011 Valladolid (Spain)
Tlf: +34 983 423566, e-mail: fernando@autom.uva.es

Abstract- In this paper, the operation of a PV system with two stages connected to the AC side of the stand-alone grid is examined. The system consists of a PV array, a boost converter, a voltage source inverter, a line AC filter, a low frequency transformer for galvanic isolation, a boost controller and an inverter controller. The boost converter controls the solar array operating point in order to track maximum power point (MPP), and the post single phase inverter controls the DC-link capacitor voltage and controls the output current to be in-phase with the grid voltage. All the components of the PV system were analyzed.

Keywords—PV System, Boost Circuit, Single Phase Voltage Source Inverter, PQ Control, Perturbation and Observation algorithm (P&O), stand alone grid.

I. INTRODUCTION

The demand for electrical energy is increasing around the world; it has motivated the use of new renewable sources of energy. Among the unconventional renewable energy sources that have been studied, PV energy is now becoming a promising economical renewable energy source, since it offers many advantages such as incurring no fuel costs, not being polluting, requiring little maintenance, and emitting no noise, among others.

The photovoltaic panel shows a non linear current-voltage characteristic varying with the irradiance and temperature which affects its power output. PV systems normally use a maximum power point tracking (MPPT) technique to continuously deliver the highest possible power when variations in the irradiance and temperature occur. In consequence, the maximum power point tracking (MPPT) control is critical for the success of a PV system. MPPT algorithms, ranging from simple hill-climbing algorithms to fuzzy logic and neural network algorithms, have been considered extensively in the literature [6].

The hill climbing algorithm is widely used in PV systems because of its simplicity. It does not require prior study or modelling of the photovoltaic panel and consider characteristics resulting from ageing, shadowing, or other operating irregularities. The basic hill climbing algorithm is the perturbation and observation algorithm (P&O) but it has oscillation problem. For that, we will consider an extended

P&O technique based on three-point weight comparison method.

Apart from MPPT technique, the core technology associated with PV systems is an “inverter” unit that converts the solar output electrically compatible with the utility grid. The inverter technology has improved from the concept of a central inverter, to string inverters, and to, for further system decentralization, AC-modules, in which every solar panel has an integrated inverter. This allows direct grid connection and provides the highest system flexibility and expandability.

One of the typical structures of the AC-module consists of two stages. The front stage performs maximum power point (MPP) tracking for maximizing the output power of the panel and voltage boost to match that of the grid. The latter grid-connected stage uses a full-bridge inverter. In common practice, energy storage elements, such as the dc-link capacitor C_{dc} , are used to compensate the difference between the dc power from the panel and the time-varying instantaneous power absorbed by the grid.

The paper is organized in the following manner: Section II introduces the basic principle of the PV system. Section III describes the P&O algorithm. Section IV shows the controller of the converter. Conclusions are finally drawn in the last section.

II. SYSTEM DESCRIPTION AND MODELLING

The description and the modeling of a PV System with two stages is described throughout this section. Figure 1 presents the basic topology of the PV System connected to the utility grid.

The boost converter controls the solar array operating point by the switch duty command, and the post single phase inverter controls the DC-link capacitor voltage and controls the output current to be in-phase with the grid voltage.

It is desirable to provide galvanic isolation between the PV System terminals and the grid. Hence, it is include a low frequency transformer at the output of the PV system.

Manuscript received June 05, 2010.

Corresponding author: J. Salazar (e-mail: johanna@autom.uva.es)

F. Tadeo (e-mail: fernando@autom.uva.es)

C. de Prada (e-mail: prada@autom.uva.es)

L. Palacin (e-mail: palacin@cta.uva.es)

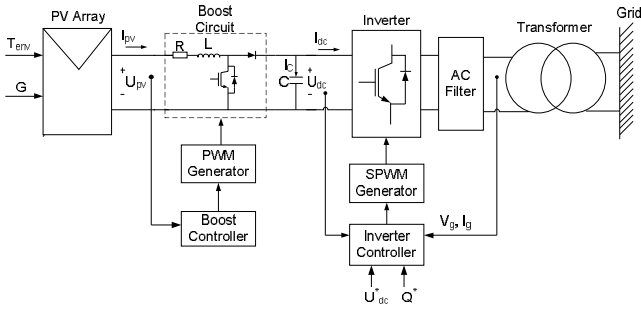


Figure 1.- Block diagram of a grid connected two stage PV System

Next, the mechanical components of the PV System as well as the boost controller, inverter controller and the electrical components (Boost Circuit and the Voltage Source Inverter) will be briefly presented.

A. Photovoltaic Panel Model

The building block of PV arrays is the solar cell, which is basically a p-n semiconductor junction that directly converts solar radiation into dc current using the photovoltaic effect. The simplest equivalent circuit of a solar cell is a current source in parallel with a diode, shown in Figure 2 [2].

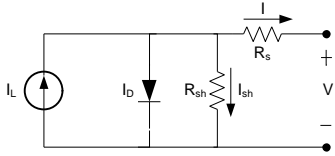


Figure 2.- Circuit diagram of a solar cell

The series resistance R_s represents the internal losses due to the current flow. Shunt resistance R_{sh} , in parallel with diode, this corresponds to the leakage current to the ground. The characteristic equation describing the photovoltaic cell is:

$$I = I_L - I_{sc} \left(\exp\left(\frac{(V + R_s I)}{V_t}\right) - 1 \right) - \frac{(V + R_s I)}{R_{sh}} \quad (1)$$

For this paper, a model of moderate complexity was used. The shunt resistance R_{sh} is neglected, I_L is approximately equal to I_{sc} and $\exp((V+R_s I)/V_t)$ is greater than 1. Also, open circuit voltage is included in the characteristic equation to comply with these conditions $I(V_{oc})=0$ and $I(V=0)=I_{sc}$. Considering the conditions above mentioned, the characteristic equation resulting is:

$$I = I_{sc} \left[1 - \exp\left(\frac{(V + R_s I - V_{oc})}{V_t}\right) \right] \quad (2)$$

PV cells are grouped together in larger units known as PV modules or arrays, which are combined in series and parallel to provide the desired output voltage and current. The mathematical model that predicts the power production of the PV array becomes an algebraically simple model, being the current-voltage relationship defined in

$$I_{pv} = I_{scg} \left[1 - \exp\left(\frac{(V_{pv} + R_{sg} I_{pv} - V_{ocg})}{V_t N_{sm} N_{sc}}\right) \right] \quad (3)$$

where

V_{pv} : Output voltage of the PV array

I_{pv} : Output current of the PV array

R_{sg} : Series resistance of the PV array

I_{scg} : Short circuit current;

V_{ocg} : Open circuit voltage

N_{sc} : Number of cells in series within the PV module

N_{sm} : Number of modules in series within the PV array

V_t : Thermal voltage

If the temperature and solar irradiation levels change, the voltage and current outputs of the PV array will follow this change. Hence, the effects of the changes in temperature and solar irradiation levels should also be included in the final PV array model. A method to include these effects in the PV array modelling is described below. According to his method, for a known temperature and a known solar irradiation level, a model is obtained.

The characteristic equation to define the module operating temperature T_c [°C] as a function of environment temperature T_{env} [°C] and solar irradiation G [W/m²] is:

$$T_c = T_{env} + G \left(\frac{NOCT - 20}{800} \right) \quad (4)$$

Where $NOCT$ is the Nominal Operation Cell Temperature, [°C], at standard test condition (STC). The testing conditions are irradiance level 1000 W/m², with the reference air mass 1,5 solar spectral irradiance distribution and module junction temperature T_{ref} of 25°C.

The variable cell operating temperature T_c affects the module open circuit voltage V_{ocm} and module short circuit current I_{scm} . These effects are represented in the model by the temperature coefficients β and α for V_{ocm} and I_{scm} , respectively, as

$$V_{ocm} = V_{ocm, stc} \left(1 + \frac{\beta(T_c - T_{ref})}{100} \right) \quad (5)$$

$$I_{scm} = \frac{I_{scm, stc} G}{1000} \left(1 + \frac{\alpha(T_c - T_{ref})}{100} \right) \quad (6)$$

Where $I_{scm, stc}$ and $V_{ocm, stc}$ are short circuit current and open circuit voltage at STC, respectively.

The simulated I-V and P-V characteristics of such a system deduced from Eq. 1 (Module GFM180, $N_{sm}=9$, $N_{pm}=3$) are represented in Figure. 3. We notice on these curves the MPP of the PV array.

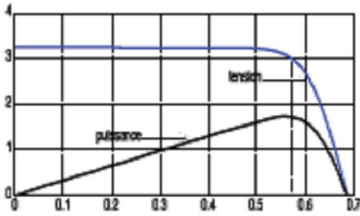


Figure 3.- I-V and P-V photovoltaic array characteristic [1]

The change of irradiance results in vertical shifting of the IV curve of the PV array as shown in Figure 4a. This change can be implemented as the shifting of the maximum operating current and the short-circuited current values. In this experiment the irradiance was changed from $200\text{W}/\text{m}^2$ to $1\text{KW}/\text{m}^2$ at constant temperature, $T=25^\circ\text{C}$. Figure 4b shows as the MPP move with the irradiation on a constant voltage.

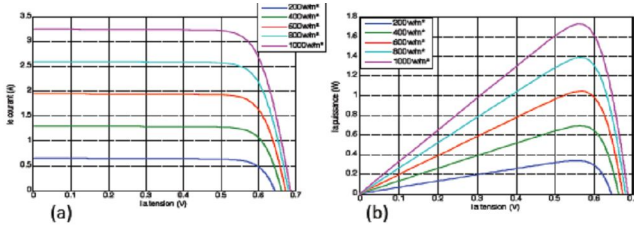


Figure 4.- Irradiation influence on PV array characteristics at constant temperature $T=25^\circ\text{C}$. (a) I-V curves, (b) P-V curves [1]

The influence of the temperature at constant irradiation, $E=1000\text{ w}/\text{m}^2$ is shown in Figure 5a. The change results in shifting the IV curve horizontally. In this experiment the temperature was changed from 0° to 75° .

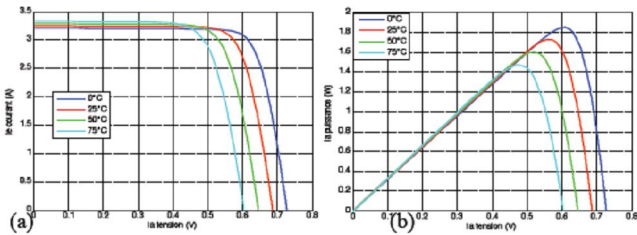


Figure 5.- Temperature dependence of the P-V characteristics at constant irradiation $E=1000\text{ w}/\text{m}^2$. (a) I-V curves, (b) P-V curves [1]

Those figures show the maximum power that can be delivered by a PV array depends greatly on irradiation and temperature. Therefore, it is necessary to track the maximum power point all the time. Many researches have been focused on various MPP control algorithm to lead the operating point of the PV array to optimum point. Among of them, the constant voltage method, the perturbation and observation (P&O) method and incremental conductance method (IncCond)

B. Boost Circuit Model

The state equation that describes boost circuit is:

$$\begin{cases} U_{pv} - RI_{pv} - L \frac{\partial I_{pv}}{\partial t} = sU_{dc} \\ I_c = C \frac{\partial U_{dc}}{\partial t} = sI_{pv} - I_{dc} \end{cases} \quad (7)$$

Where, L is storage inductance, C is capacitor, R is resistance of inductance, U_{pv} is output voltage of the PV array, I_c is capacitor current, I_{dc} is output current of boost circuit, that is, the current injected into the single phase inverter, s is the switch status.

$$s = \begin{cases} 0 & \text{IGBT close} \\ 1 & \text{IGBT open} \end{cases} \quad (8)$$

The current supplied by boost circuit model is discontinuous. Thus, a larger filter capacitor is required to limit the output voltage ripple. The filter capacitor must provide the output dc current to the load when the diode is off. If the capacitor is larger, the output voltage ripple will be reduced, system response will be slower and the capacitor cost will increase

B. Single Phase Voltage Source Inverter (VSI) Model

A single-phase inverter is shown in Figure 6; where U_{dc} is the voltages of the dc bus capacitors; U_{ac} is the phase voltage and each switch is identified with the letter Q . It is assumed that Q_1 and Q_2 as well as Q_3 and Q_4 are switched in a complementary way to avoid a short circuit in the voltage source. Thus, the analysis of the switches turn-ons/off is simplified. We only consider the switches of the two upper transistors Q_1 and Q_3 . If the switch of the transistors Q_1 is on, then Q_1 is equal to 1 and vice versa. As we have two variables, there are ($2^2=4$) possible switching vectors; they are showed in Table I.

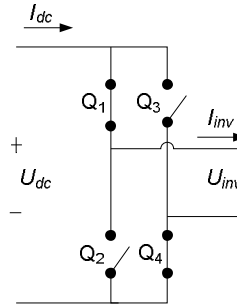


Figure 6.- Structure of the single phase voltage source converter

The applied voltages at the AC filter terminals as a function of the DC-link voltage and the switching functions is:

State	Q_1	Q_3	U_{inv}
1	1	0	U_{dc}
2	0	1	$-U_{dc}$
3	1	1	0
4	0	0	0

Due to the fact that the inverter is assumed lossless and constructed without storage energy components, the instantaneous power balance indicates that:

$$U_{dc} I_{dc} = U_{inv} I_{inv} \quad (9)$$

The output current AC I_{inv} is taken from AC Filter. The output voltage U_{inv} is considered sinusoidal. The dc link voltage remains constant U_{dc} . The dc link current I_{dc} is given by:

$$I_{dc} = \frac{U_{inv} I_{inv}}{U_{dc}} \quad (10)$$

Several modulating techniques have been developed that are applicable to full-bridge VSIs. Among them are the PWM (bipolar and unipolar) techniques.

D. AC Filter Model

The line filter reduces the high frequency harmonic content of the line current caused by the switched operation of the VSI.

Usually, the line filter consists of filter inductors but other combinations of capacitors and inductors such as LC- or LCL filters can be used.

The L-filter is a first-order filter. Its attenuation is 20 dB/decade over the whole range of frequency. Using this filter, the switching frequency of the converter has to be high to obtain sufficient attenuation of the harmonics caused by the PWM converter.

The LCL filter (Figure 7) is a third-order filter. Its attenuation is 60 dB/decade for frequencies over the resonance frequency. it is possible of using a relatively low switching frequency [4].

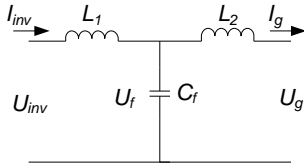


Figure 7.- LCL Filter Single Phase Case

The mathematical model of the LCL-filter is given by:

$$U_{inv} = L_1 \frac{\partial I_{inv}}{\partial t} + U_f \quad (11)$$

$$U_f = L_2 \frac{\partial I_g}{\partial t} + U_g \quad (12)$$

$$C \frac{\partial U_f}{\partial t} = I_{inv} - I_g \quad (13)$$

III. PERTURBATION AND OBSERVATION ALGORITHM

The Perturbation and Observation algorithm (P&O) is the most popular MPPT algorithm due to its simplicity. Figure 1 shows the flow chart of P&O method. It operates by disturbing the voltage of the panel periodically, and by comparing the energy previously delivered with those after disturbance. The principle can be described as follow: If a given perturbation on the voltage of the panel leads to an increase (decrease) the output power of the PV, then the subsequent perturbation is generated in the same (opposite) direction. As a consequence of the principle of the P&O algorithms, when the MPP is reached, the system will oscillate around it. The oscillation can be minimized by reducing the perturbation step size. However, a smaller perturbation size slows down the MPPT.

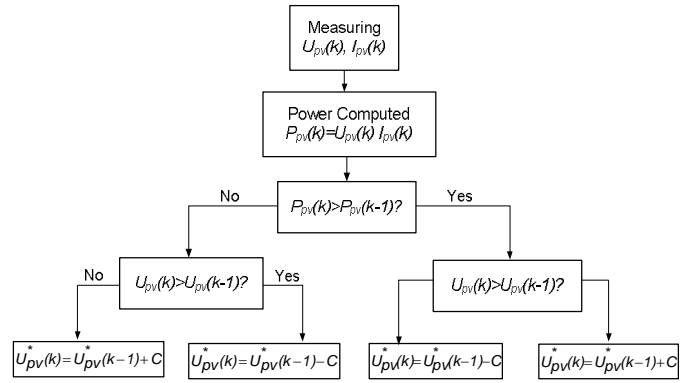


Figure 5.- The flow chart of P&O method [3]

The P&O method works well in slow changing environment but has some limitations under rapidly changing atmospheric conditions as illustrated in Figure. 8. Starting from an operating point A, if atmospheric conditions stay approximately constant, a perturbation ΔV in the PV voltage V will bring the operating point to B and the perturbation will be reversed due to a decrease in power. However if the irradiance increases and shifts the power curve from P_1 to P_2 within one sampling period, the operating point will move from A to C. This represents an increase in power and the perturbation is kept the same. Consequently, the operating point diverges from the MPP and will keep diverging if the irradiance steadily increases. The P&O algorithm deviates from the MPP until a slow solar radiation change occurs or settles down

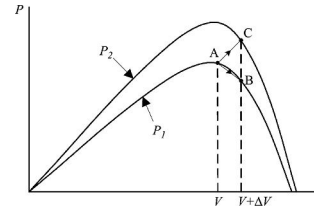


Figure 8.- Divergence of P&O from MPP as shown in [5].

IV. MODEL OF CONTROLLERS

A. Boost controller model

The control scheme is shown in Figure 9. Frequency Shift Power control defined percentage of output power ($\%P_{ac}$) as a function of grid frequency deviation. Cross coupling switch must able to choose between power optimization and power limitation depending on $\%P_{ac}$. Power optimization is refers to MPP tracking. It leads the operating point of the PV array to optimum point in order to deliver the highest possible power. Power limitation regulates output power from PV System depending on $\%P_{ac}$. Both Power optimization and Power limitations produces a reference voltage which is compared with output voltage PV array. This difference is the input to the PI controller which controls PWM generator.

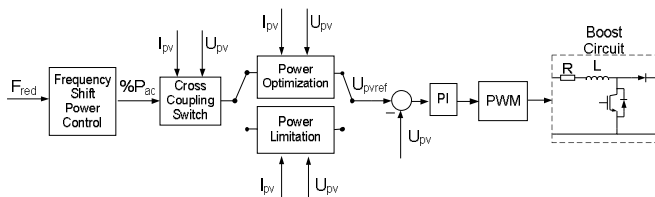


Figure 9.- Boost Controller Model

Frequency Shift Power Control

If PV System is connected to the AC side of the stand-alone grid (see figure 10), battery inverter must be able to inform to the PV System when it must limit its output power in order to prevent the excess energy from overcharging the battery. The communication language is frequency. In other words, the battery inverter recognizes this situation and changes the frequency at the AC output. This frequency is analysed by PV System which limits its output power according to the frequency previously defined by battery inverter. The operating principle used by PV system is called Frequency Shift Power Control (FSPC) [7]. This function is shown in the Figure 11, for more information read Sunny Island 5048 Manual

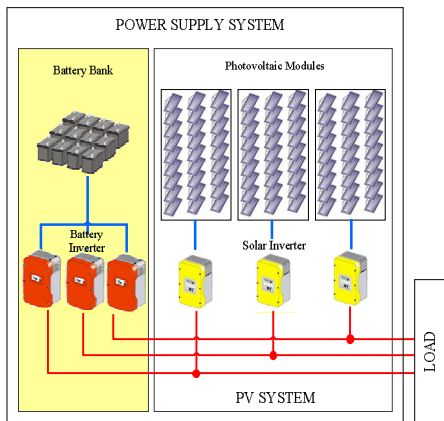


Figure 10.- Block diagram of a stand-alone grid

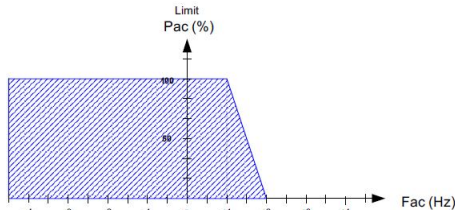


Figure 11.- Frequency Shift Power Control

f_0 refers to the base frequency of the stand- alone grid, in our case, it is equal to 50Hz. When the grid frequency deviation is less than 1 Hz and higher than -5Hz, $\%P_{ac}$ is equal to 100%; when a grid frequency deviation occurs between 1 and 2 Hz, $\%P_{ac}$ is different from 100% and when the grid frequency deviation is higher than 2 Hz, $\%P_{ac}$ is equal to 0%.

Switch Cross Coupling

If $\%P_{ac}$ is fixed at 100, then switch cross coupling will chose *Power Optimization*. When a grid frequency deviation between 1 and 2 Hz occurs, switch cross coupling will sense current and voltage output in order to compute the limit power P_{lim} . At this moment, the current power is obviously higher than limit power, then switch cross coupling will chose *Power Limitation*. The switch cross coupling keeps this option until the current power will be lower than P_{lim} . At this moment, switch cross coupling leaves to introduce change. If a changing environment occurs in such a way that the current power is lower than $0.8P_{lim}$, switch cross coupling will chose *Power Optimization* in order to increase power supply. switch cross coupling keeps this option, as long as the current power keeps below $0.8P_{lim}$. When the current power is equal or higher than $0.8P_{lim}$, switch cross coupling will leave to introduce change. The flow chart is shown below:

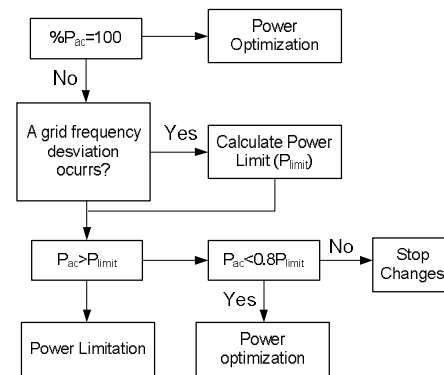


Figure 12.- The flow chart of Switch Cross Coupling

Power Limitation

It operates by disturbing the voltage of the panel periodically, and by comparing the energy previously delivered with those after disturbance. The principle can be described as follow: If a given perturbation on the voltage of the panel leads to a decrease (increased) the output power of the PV, then the subsequent perturbation is generated in the same (opposite) direction. It keeps doing it until the current output power is lower than limit power P_{lim} .

V. CONCLUSION

This work shows the performance of a PV system grid connected through a single voltage source inverter. PV array output voltage is converted into DC voltage through a Boost DC converter, and then it is converted into AC voltage through a single Voltage Source Inverter (VSI). The Boost circuit controller is used to regulate output power; the inverter controller is used to control dc-link voltage. The DC-link capacitor voltage is maintained at a constant value by ensuring the balance of the input and output energy of the both sides of the capacitor. The future work will be simulate the whole system and compare this result with typical configurations.

REFERENCE

- [1] Abdallah Zegaoui, Pierre Petit, Jean Paul Sawicki, Jean Pierre Charles, Michel Aillerie, M. Della Rachai & A.O. Belarbi. “*Simulation of Photovoltaic Generators and Comparison of two common Maximum Power Point trackers*”. International Conference on Renewable Energies and Power Quality (ICREPQ'10)
- [2] A. Chouder, S. Silvestre and A. Malek. “*Simulation of photovoltaic grid connected inverter in case of grid-failure*”. Revue des Energies Renouvelables, Vol. 9 N°4 (2006) 285 – 296
- [3] A. Yafaoui., B. Wu and R. Cheung. “*Implementation of Maximum Power Point Tracking Algorithm for Residential Photovoltaic systems*”. 2nd Canadian Solar Buildings Conference Calgary, June 10 – 14, 2007
- [4] Fei Liu¹, Xiaoming Zha¹, Yan Zhou², Shanxu Duan. “*Design and Research on Parameter of LCL Filter in Three-Phase Grid-Connected Inverter*” IEEE 2009
- [5] O. Wasynczuk, “*Dynamic behavior of a class of photovoltaic power systems,*” IEEE Trans. Power App. Syst., vol. 102, no. 9, pp. 3031–3037, Sep. 1983.
- [6] Trishan Esum and Patrick L. Chapman. “*Comparison of Photovoltaic Array Maximum Power Point Tracking Techniques*” IEEE Transactions on Energy conversion, Vol 22, N° 2, June 2007 439.
- [7] Sunny Island SI 5048 “*Installation & Instruction Manual*”